Practical considerations in realizing a magnetic centrifugal mass filter

Renaud Gueroult and Nathaniel J. Fisch
Princeton Plasma Physics Laboratory, Princeton University, Princeton, New Jersey 08543, USA

(Received 30 May 2012; accepted 26 November 2012; published online 12 December 2012)

The magnetic centrifugal mass filter concept represents a variation on the plasma centrifuge, with applications that are particularly promising for high-throughput separation of ions with large mass differences. A number of considerations, however, constrain the parameter space in which this device operates best. The rotation speed, magnetic field intensity, and ion temperature are constrained by the ion confinement requirements. Collisions must also be large enough to eject ions, but small enough not to eject them too quickly. The existence of favorable regimes meeting these constraints is demonstrated by a single-particle orbit code. As an example of interest, it is shown that separation factors of about 2.3 are achievable in a single pass when separating Aluminum from Strontium ions. © *2012 American Institute of Physics*. [http://dx.doi.org/10.1063/1.4771674]

I. INTRODUCTION

Rotating plasma configurations have long been identified as promising techniques to discriminate elements depending on their mass.[1] Although most of the past studies have been devoted to isotope separation,[2–5] in the last decade plasma mass separation techniques have attracted interest for processing nuclear waste,[6,7] for which the mass discrimination requirement is less severe. This high-throughput application relies upon the fact that the costs of ionization are small compared with the cost of chemical separation. In particular, in the Ohkawa mass filter, particles are separated relying on a charge to mass ratio threshold value for ion radial confinement.[6]

In the Ohkawa filter, as well as in other separation devices based on centrifugal forces, the unconfined heavy stream is collected at the radial outer surfaces, which makes more difficult the collection of the heavy elements. It would be advantageous, therefore, to collect the ions axially rather than radially. An alternative plasma separation mechanism solves this issue by producing two confined axial output streams.[8] Called the *magnetic centrifugal mass filter* (MCMF), it features ions that are extracted axially, that is to say along magnetic field lines. The separation is achieved in a collisional rotating cylindrical plasma with asymmetric confinement properties at each end. At one end, the confinement is dominated by magnetic forces, which are independent of mass, like in a magnetic mirror. At the other end, the confinement is dominated by centrifugal forces, which are proportional to the mass. Although this mass separation concept has promising characteristics, and it may compare favorably to the Ohkawa filter,[9] its potential for nuclear waste processing has not been analyzed in detail. In particular, the technique will depend on whether a parameter space of favorable operating conditions can actually be found for a set of self-consistent operating conditions, such as number densities, temperatures, and rotation speeds.

In this paper, the physical processes responsible of the existence of a mass separation effect in a magnetic centrifugal mass filter are analyzed with the purpose of marking the practical operating parameter space boundaries. First in Sec. II, the physical phenomena responsible of the mass separation effect are introduced. These phenomena constrain the parameter space for mass separation. In Sec. III, the existence of favorable separation regimes is demonstrated using a single-particle simulation. In Sec. IV, the main findings are summarized.

II. OPERATIONAL REGIME BOUNDARIES

To assess the MCMF device, we first review the mass separation physical mechanisms. The ion temperature T_i the rotation speed, magnetic field intensity, the plasma density, all affect the separation effect. The ion temperature is assumed here to be a free parameter with respect to the rotation speed, and is chosen independent of the ion mass. The justification of these assumptions will be discussed in Sec. II B addressing the influence of collisions.

A. Confinement requirements

The MCMF is illustrated schematically in Figure 1. The plasma rotation could in principle be achieved by placing concentric electrodes[10] at each end of the device, so as to control the electric potential distribution and in turn the $\mathbf{E} \times \mathbf{B}$ drift speed. Another option, yet to be demonstrated experimentally, would be to rely on wave induced rotation.[11]

The ion confinement on the *light-element side* (right side in Figure 1) results from centrifugal forces. These centrifugal forces restrain heavy ion but not light ions, so that it is the light species that tends to exit preferentially on this *light-element side*. Therefore, the ion thermal kinetic energy should be such that heavy ions cannot overcome the centrifugal potential well. On the other hand, since light ions are to be extracted at this end, the ion thermal kinetic energy should be higher than, or at least of the order of, the centrifugal potential barrier for light ions. Both conditions can be satisfied by properly tuning the rotation speed, since the centrifugal potential well is deeper for heavier elements.

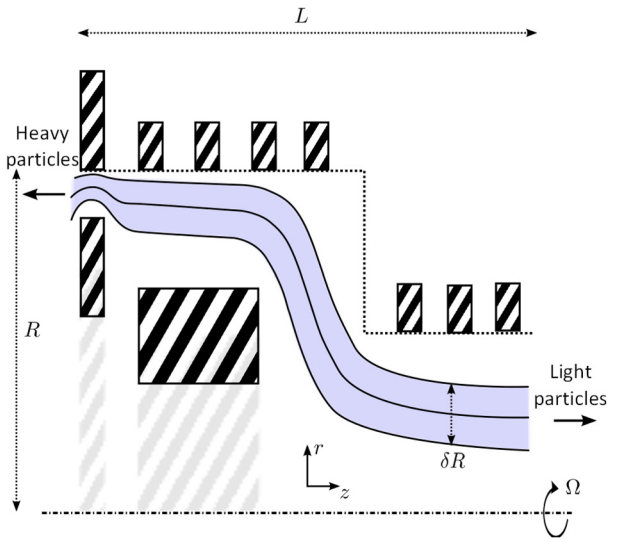

FIG. 1. MCMF typical configuration. Solid lines represent magnetic field lines; the dashed line represents the vacuum boundary; the dashed-dotted line indicates the axis of symmetry; hatched boxes represent magnetic field coils and the shaded region indicates the particle confinement region.

For rotation frequencies Ω much smaller than the cyclotron frequency ω_c, the additional azimuthal drift induced by centrifugal forces is negligible,[1] so that the rotating speed can be reasonably approximated by the azimuthal $\mathbf{E}\times\mathbf{B}$ drift velocity. Introducing r_0 the ion initial radial position and r_{m_L} the radius of the same magnetic line at the light side, the ion confinement condition on the light element side then reads

$$\frac{m_L}{2}(1-R_{R_L}^{-1})\Omega^2 r_0^2 \geq T_i, \tag{1a}$$

$$\frac{m_H}{2}(1-R_{R_L}^{-1})\Omega^2 r_0^2 \leq T_i, \tag{1b}$$

where m_L and m_H are, respectively, the light and heavy ion masses, and $R_{R_L}=(r_0/r_{m_L})^2 \geq 1$ is the light-side radius ratio. For ion temperatures of the order of 10 eV and for ion species of particular interest for waste remediation, such as iron or strontium, these two conditions lead to rotation speeds of a few km s^{-1} to tens of km s^{-1}.

Consider now confinement on the *heavy element side*, the left side in Figure 1, where it is the heavy species that leaves preferentially. The light species in confined at this end by the magnetic mirror force. Assuming identical temperature T_i for the various ionic species, their magnetic moment μ is the same, and the mass separation effect thus results because of the larger parallel speed heavy ions gain by drifting into a deeper centrifugal potential well. The confinement condition for an ion created inside the device at (r_0, z_0) with zero parallel kinetic energy—for example by electron impact ionization—is then

$$\mu B_0(R_{B_H}{}^{-1}-1) \geq \frac{m_L}{2}(R_{R_H}{}^{-1}-1)\Omega^2 r_0^2, \tag{2}$$

with $R_{B_H}=B_0/B_{m_H}\leq 1$ the ratio of the magnetic field B_0 at the ion initial position (r_0, z_0), to the maximum heavy-side magnetic field B_{m_H}. Similarly, we define the heavy side radius ratio $R_{R_H}=(r_0/r_{m_H})^2 \leq 1$, where r_{m_H} is the radius at the heavy-side magnetic mirror of the magnetic field line passing by the ion initial position (r_0, z_0).

An immediate consequence of confinement conditions (2a) and (2b) is that the confinement of a given ion species at each end of the system will strongly depend on the radial position where the ion is created. The radial positions available of course change with axial position. As shown in Fig. 2, initializing an ion closer to the light element side $(r_0' = r_0 - \delta r_0)$ will decrease the confinement at both ends. Note that the initial velocity of an ion is largely perpendicular and with the local rotation speed in the rotating frame. Thus, the confinement is decreased at the light-element side because, ionized at lower radius, there is less centrifugal force to overcome in leaving on the light-element side. On the other hand, the confinement is also decreased at the heavy-element side because, ionized at lower radius and therefore lower rotation speed, the perpendicular energy (or magnetic moment) is smaller in the rotating frame, so the magnetic confinement at the heavy-element side is less effective.

Specifically, although the light-side loss cone area increase is the larger one, with a decrease of the parallel velocity required to overcome the centrifugal potential well

$$\delta v_\parallel^c \sim -\frac{\Omega\delta r_0}{\sqrt{1-R_{R_L}{}^{-1}}}\left(1-\frac{\delta r_0}{r_0}\right), \tag{3}$$

the heavy side loss cone area increases as well due to the larger parallel energy gained by ions in response to the larger radial displacement $r_{m_H}-r_0'$. Ion confinement on the heavy element side therefore requires higher perpendicular velocity

$$\delta v_\perp{}^c(v_\parallel=0) \sim \frac{\Omega\delta r_0}{\sqrt{(R_{B_H}{}^{-1}-1)(R_{R_H}{}^{-1}-1)}}\left(1-\frac{\delta r_0}{r_0}\right), \tag{4}$$

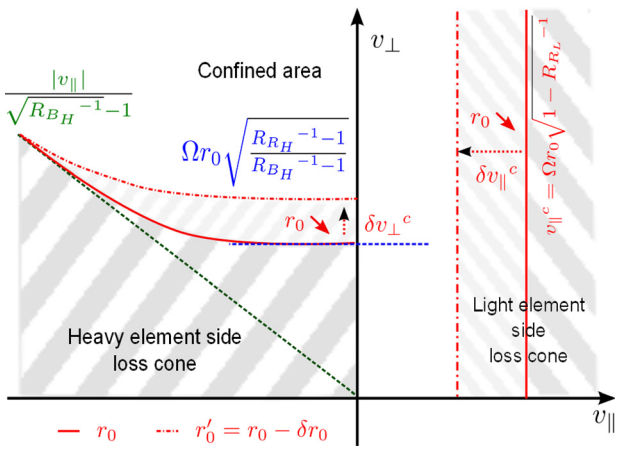

FIG. 2. Evolution of the loss cones shapes as a result of a decrease of the initial radial position r_0 to $r_0'=r_0-\delta r_0$. $R_{B_H}=B_0/B_{m_H}\leq 1, R_{R_H}=(r_0/r_{m_H})^2 \leq 1, R_{R_L}=(r_0/r_{m_L})^2 \geq 1$. Confinement on both sides decreases. The parallel velocity corresponding to ion confinement on the light element side decreases by $\delta v_\parallel{}^c$, making the ion more likely to leave on the light element side. In the meantime, the minimal perpendicular velocity allowing confinement on the heavy element side increases by $\delta v_\perp{}^c$.

that is a larger magnetic moment, to balance this effect. The region where plasma constituents are to be injected can thus be expected to play an important role in mass separation.

The magnetic field intensity is also constrained from the requirement that ions be magnetized. Since ions produced by ionization have a velocity close to the $v_{\mathbf{E}\times\mathbf{B}}$ drift velocity in the frame rotating at the angular frequency $E/(Br)$, the magnetic field intensity required to ensure ion magnetization is a function of the rotation speed. The ion gyroradius should be much smaller than the radial dimensions of the device, in order to accommodate collisional diffusion that results in axial extraction but not radial extraction. For example, for a device with radius on the order of centimeters, at $v_{\mathbf{E}\times\mathbf{B}} = 6\ \mathrm{km\,s^{-1}}$, a magnetic field of 2 T is required to limit the gyroradius $r_L = mv_{\mathbf{E}\times\mathbf{B}}/(eB_0)$ of a strontium ion to values lower than 3 mm.

B. Collisional effects influence

Collisional considerations yield two distinct requirements delimiting the achievable ion and electron number densities domain.

The first one is a direct consequence that ion extraction on the light element side requires a parallel velocity component allowing the ion to reach radial positions lower than the initial position r_0. Since the ion velocity in the rotating frame is initially purely azimuthal, for ions to leave on the light element side requires a redirection of the velocity vector through ion-ion pitch angle scattering. On the other hand, too much slowing down would yield a loss of magnetic confinement of light elements on the heavy element side. Also, the ion slowing down time should be longer than the typical ion bounce period, otherwise the ion magnetic moment will decrease below the threshold value for magnetic mirror reflection, and light ions will be lost on the heavy element side. Consequently, the operating parameters need to be chosen such that ion-ion collisional phenomenon are reasonably predominant over ion-electron ones, limiting in turn the ion slowing down to its ion-ion component. For a singly charged ion of mass m, and assuming that $m\Omega^2 r_0^2 \gg T_i$, this condition implies[12]

$$\frac{m\Omega^2 r_0^2}{2eT_e} \leq 10\left(\frac{n_i}{n_e}\sqrt{\frac{m}{m_p}}\right)^{2/3}, \tag{5}$$

where m_p is the proton mass and T_e is in electron-volt. Initial ion energy being proportional to mass, Eq. (5) is more stringent for heavy ions, meaning that for a given set of operating conditions (rotating speed, electron temperature, and number densities), the lighter the ion the more likely that ion-ion collisions dominate ion-electron collisions.

The second requirement results from the axial output stream feature of the MCMF. When collisionality increases, ion diffusion perpendicular to the magnetic field lines increases, which limits the ability of the system to produce a well confined output stream. Consequently, even if the ion-electron collision rates are low as stated in Eq. (5), one would have to ensure that the perpendicular diffusion due to ion-ion collisions is sufficiently small compared to the inverse of the typical ion residence time so that perpendicular displacement induced by perpendicular diffusion remains limited compared to parallel one. Practically, this requirement relates the ion number density to the ion temperature and the rotating speed.

The parameter regime identified above is such that the ion-ion velocity diffusion time $\tau_\perp^{i|i}$ is shorter than both the ion-electron slowing down time $\tau_\nu^{i|e}$ and the bounce time. Since the inter-species ion-ion relaxation time $\tau_\epsilon^{i|i'}$ is of the same order of magnitude as the intra-species ion-ion velocity diffusion times $\tau_\perp^{i|i}$ and $\tau_\perp^{i'|i'}$ for moderate $m_{i'}/m_i$ ratios ($\sim$1.5 for the case of Strontium and Iron ions of interest for waste remediation), a kinetic energy transfer will exist between light and heavy elements. The ratio of the heavy to light ion kinetic energy $\varepsilon_H/\varepsilon_L$ will decrease (starting from its initial value m_H/m_L) towards one on the timescale corresponding to the ion redirection parallel to the magnetic field lines. This trend motivates the assumption of the mass-independent ion temperature previously used. For $\varepsilon_H/\varepsilon_L < m_H/m_L$, light ions will be more easily collected on the light side than heavy ones. On the other hand, as their magnetic moment decreases, heavy ions will more easily exit through the heavy side. The opposite effect—increase of the magnetic moment together with the increase of the confinement on the heavy side—will be observed for light ions.

In addition to the ion inter-species collisions effects, the ion temperature will decrease as a result of ion-electron and ion-neutral collisions. The ion temperature may also be independently increased by means of external heating mechanism (for example using radio frequency waves[7]). Predicting the ion temperature for a given rotation speed is therefore not trivial, and will anyway depend on other technological parameters. For this reason, although the ion temperature is chosen within a reasonable range around the rotation energy, the two parameters are otherwise considered as independent within the practical parameter space considered.

To summarize, the desired ion temperature dictates the device rotation speed, which in turn dictates the magnetic field intensity. In addition, collisions tie the rotation speed to both the electron and ion number densities, while the axial collection capability limits the collision rate.

III. ESTIMATE OF THE MASS SEPARATION EFFECT

Having outlined the operating parameter space boundaries for the MCMF, we now evaluate the achievable mass separation of this device. A single particle numerical model is developed to first demonstrate the mass separation effect under the previously identified operating conditions, and then to develop a better understanding of the separation phenomena.

A. Numerical model

The numerical approach consists of computing the trajectories of a large number of independent singly-charged ions interacting with a background plasma of electrons, similar ions, and parent neutrals. Ions trajectories are followed until the ion exits the computational domain.

As a pre-processing step, after choosing a magnetic field configuration such as the one sketched in Fig. 1, a magnetostatic solver is called to obtain the corresponding magnetic field map. The field solution, as pictured in Fig. 3, is then used as an input for the simulation. Next, magnetic field lines are used to compute the electric field assuming that magnetic field lines form equipotential surfaces. Space charge effects are neglected. More specifically, for magnetic field lines originating from the heavy element side, the electric potential decreases linearly with the radial coordinate along the domain boundary.

Coulomb collisions are modeled in a Langevin formalism,[13] assuming homogeneous and isotropic distributions of background ions and electrons. Ion-neutral collisions—elastic and charge exchange collisions—are simulated by means of a Monte-Carlo model.[14] Due to the lack of cross section data in the literature for heavy ion (iron, strontium) elastic and charge exchange impact on its parent atom, the same energy independent cross section ($\sigma = 10^{-19}\,\mathrm{m}^2$) is used for both processes. Such values are of the order of charge exchange cross section for low energy iron ion on hydrogen atom.[15] Although the use of an arbitrary cross section value forbids quantitative estimates of the background gas effects as function of the pressure, it is sufficient for a qualitative study. An overestimation of the cross section is equivalent to an underestimation of the neutral number density and vice-versa, since it is the product of these two parameters that determines the mean free path. Ion-ion and ion-electron collision rates and scattering are computed in the rotating frame, while ion-neutral collisions are computed in the reference frame.

Ion trajectories are computed in the reference frame using a modified fourth order Runge-Kutta algorithm[16] and choosing a time step Δt sufficiently small ($\Delta t \sim 2\pi/(20\ \omega_c)$) to ensure energy conservation over the simulation duration. Vector fields value at particle position is linearly interpolated from 100×120 grid-based discrete data.

Since the optimal method of waste introduction is still to be determined, the ion source profile is not now known. Our approach, therefore, is to consider a point source at a given location (r_0, z_0), and to parametrically study the sensitivity of the mass separation on this location. Once a specific particle injection mechanism is determined, the mass separation performance of the device could then be deduced by integrating over the corresponding ion source profile.

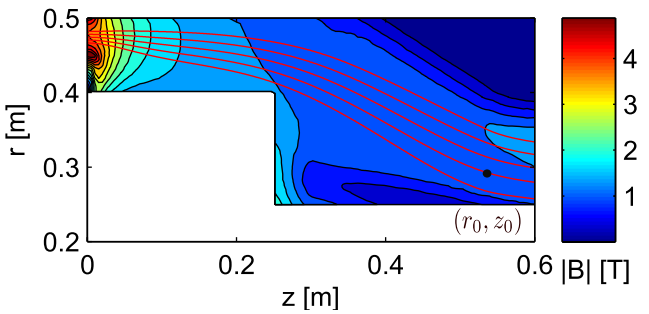

FIG. 3. Magnetic field solution in the (r, z) plane used as input data for 3D ion trajectory simulation.

B. Mass separation effect

Figure 4 presents typical simulation results obtained for an initial position (r_0, z_0) such that operating conditions satisfy constraints (1), (2), and (5). The mass separation effect is apparent; approximatively 0.4 aluminum ions are collected at the heavy element side for one aluminum ion collected at the light element side, while the same ratio increases with ion mass up to 1.65 in case of strontium ions.

Additionally, these results indicate an increase of the radial losses with ion mass. These losses represent as much as 14% of the ion outward flux for strontium ions. As pointed out above, this trend results from the perpendicular displacement when ions suffer collisions. This displacement is of the order of the Larmor radius, *i.e.* proportional to the ion mass, so that radial losses are larger for heavier elements. It should be noted here that, while these radial losses are undesirable, optimizing the magnetic field shape, or making the system larger in radius, should reduce the radially-lost ion population, eventually maximizing the heavy element separation factor.

C. Parameter space search

It is important to maximize the ratio of light to heavy mass ions collected on the light side, and similarly, to maximize the ratio of heavy mass ions to light mass ions collected on the heavy side. At the same time, it is important to minimize radial losses. The operating parameter space around the base case conditions corresponding to Fig. 4 is explored numerically, by varying successively the ion temperature, the electron temperature, the rotation speed, the neutral number density and the charged particle number density, as shown in Table I.

Cases *A*, *B*, and *C* depicted in Fig. 5 illustrate the dependence of the mass separation on the ion temperature. An

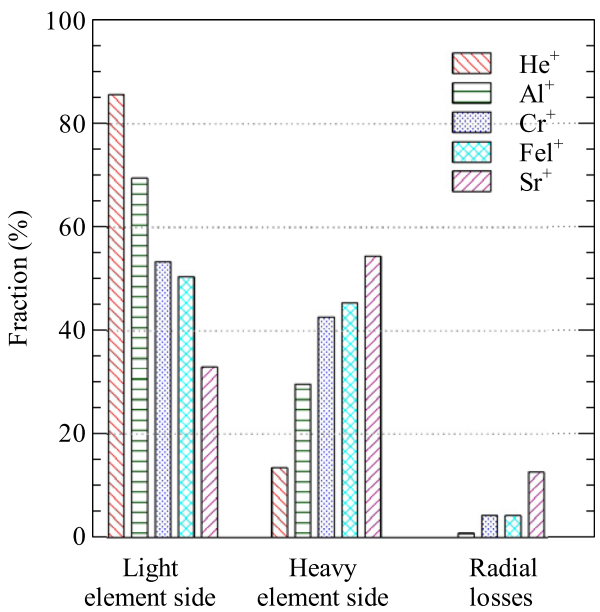

FIG. 4. Typical computed ion fluxes. $n_e = n_i = 1.5\ 10^{12}\,\mathrm{cm}^{-3}$, $T_i = 20\,\mathrm{eV}$, $T_e = 2\,\mathrm{eV}$, $v_{\mathbf{E}\times\mathbf{B}} = 8.5\ \mathrm{km.s}^{-1}$, $n_n = 0$. Results show a mass separation effect, with light ions mainly collected on the light element side while most of the heavy ions get to the heavy element side. Radial losses increase with ion mass because of the larger Larmor radius of heavy ions.

TABLE I. Operating conditions used for single particle simulations.

	Case *A*	Case *B*	Case *C*	Case *D*	Case *E*	Case *F*	Case *G*	Case *H*
T_e (eV)	2	2	2	0.2	2	2	2	2
T_i (eV)	20	10	30	20	20	20	20	20
$n_e = n_i$ ($\times 10^{12}$ cm^{-3})	1.5	1.5	1.5	1.5	1.5	1.5	1.5	4.5
$v_{E\times B}$ (km s^{-1})	8.5	8.5	8.5	8.5	10.6	8.5	8.5	8.5
σn_n (m^{-1})	0	0	0	0	0	0.1	0.5	0

increase of the ion temperature T_i enhances ion collection at the light element side at the expense of both the heavy element side and the radial losses. Apparently, the higher ion temperature produces a higher magnetic moment, and thus a better ion confinement on the heavy element side. At the same time, although the higher ion temperature reduces collisions so that scattering rate of ions to the light side loss cone decreases, the larger ion parallel kinetic energy after scattering eases the ion collection on the light element side. This interpretation, however, does not inform on the radial losses. For a given initial ion kinetic energy; that is to say rotation speed, increasing the background ion temperature T_i will result in a decrease of the ion-ion slowing down rate, in a decrease of the ion-ion perpendicular diffusion rate but in an increase of the parallel diffusion rate. Since the parallel diffusion rate is lower than both the perpendicular diffusion and the slowing down rates, the overall decrease in collisional rates explains the observed decrease of the radial losses.

The dependency of the mass separation factor on the electron temperature T_e (cases *A* and *D*) can be explained similarly. The perpendicular and parallel diffusion rates are negligible compared to the slowing down rate for ion-electron collisions. Thus, decreasing the electron temperature increases the ion-electron slowing down rate. This increases the ion collection on the heavy element side since the ion confinement on the heavy element side is decreased because of the diminishing ion magnetic moment. The ion collection on the light element side is consequently reduced because of a weaker reflection of ions on the heavy element side. At the same time, the increase in the ion-electron slowing down rate enhances the radial losses. This trend is strengthened, as stated in Eq. (5), by the decrease of the ion-ion collisions predominance over ion-electron ones triggered by a decrease of the electron temperature T_e.

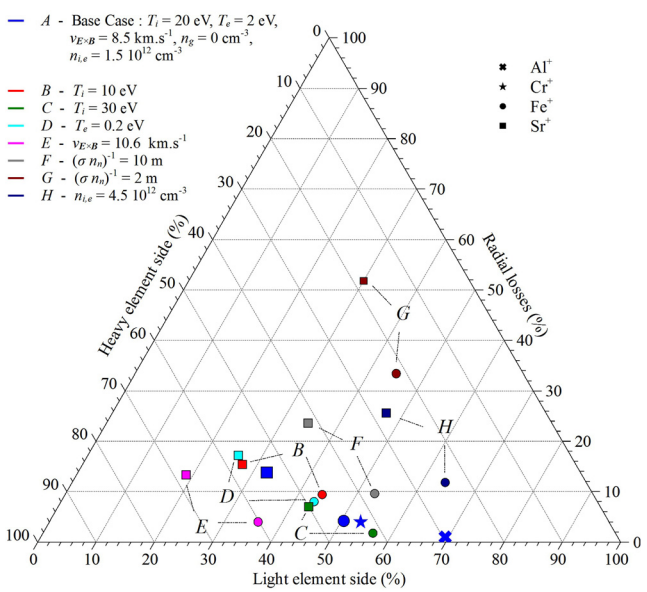

FIG. 5. Separation factor for various operating conditions summarized in Table I.

All other things being equal, the effect of a rotation speed increase is quite straightforward. A larger rotation speed makes the centrifugal potential well deeper, making it harder for ions having a given temperature to overcome the corresponding potential barrier toward the light element side. On the other hand, this deeper centrifugal potential well increases the parallel kinetic energy gained by ions on their way to the heavy side magnetic mirror, limiting the fraction of reflected ions. An increase of the rotation speed consequently results in a decrease of collection on the light element side and an increase on the heavy element side. Assuming that the ion thermalization is faster than all other collisional processes, the rotation speed does not impact the radial losses, as illustrated by cases *A* and *E* in Fig. 5.

As shown by comparing cases *A*, *F*, and *G* in Fig. 5, the separation factor as a function of the background neutral gas number density can be divided into two regimes. For limited values of σn_n (the inverse of the mean free path); the ion-neutral collisions increase both the collection of ions on the light element side, because of a higher scattering rate for velocity deflection, and the radial losses at the expense of the heavy element side stream. On the other hand, when the mean free path becomes lower than the typical distance an ion has to cover along its helical path to reach the light element side, the ion collection on the light element side starts decreasing as well. Consequently, for shorter mean free paths, the radial losses increase at the expense of both the heavy and light element side streams.

The effect of increasing the charged particle number density is qualitatively similar to the effect of increasing the neutral number density. Since the Coulomb collision rates are proportional to density, an increase in density increases both the light element side collection and the radial losses at the expense of the heavy element side collection (cases *A* and *H*). Note that the ratio of light element side ion collection to radial losses is greater when collisions arise from charged particles as opposed to background neutral gas. An explanation of this difference lies in the different nature of charge exchange and Coulomb collision; charge exchange collisions induce an ion mean perpendicular displacement equal to one gyro-radius for each collisional event, while Coulomb collisions yield on average a smaller perpendicular

displacement. In addition, in a similar manner as for ion-neutral collisions, the light element side stream is expected to decrease in favor of radial losses above a given charged particle number density.

To summarize, the mass separation effect can be produced over a rather large parameter range. More specifically, the centrifugal barrier can be strengthened by increasing the rotation speed. This will minimize the appearance of heavy ions in the light element side stream. On the other hand, collisions increase the collection of ions on the light element side. An increase of the ion temperature similarly increases the collection on the light element side, but without the undesired increase of radial losses.

The plasma composition is expected to play an important role on the mass separation effect, because of the mass dependence exhibited by the collision rates. Indeed, the light ions will be more easily deflected upon interacting with heavier ions, while heavier ion deflection will be reduced. Thus light ions will be more easily collected, as desired, on the light element side. Preliminary numerical simulation results confirm this mass separation enhancement.

IV. SUMMARY

Although not every physical effect was considered (such as radiation losses and space charge effect), the key issues in determining a parameter range for operating the MCMF were addressed. In particular, the main physical phenomena yielding a mass separation effect in a MCMF were addressed with the purpose of (i) identifying the nominal operating conditions for the realization of such a device and (ii) estimating the achievable mass separation capabilities of this concept.

The densities suitable for operating this device have been shown to be primarily constrained by collisions. First, collisions have to be sufficiently large so that ions can be efficiently scattered into the light element side loss cone. This condition sets a density minimum, under which ion collection on the light element side is not achievable. On the other hand, the higher the collisionality, the larger are the undesired radial losses for a given geometric configuration. As a matter of fact, radiation losses set another density upper limit, but this condition is expected to be less stringent than the one induced by collisions for the considered electron temperature and plasma composition. Although collisionality depends on the ion and electron temperatures, we demonstrated that number densities of a few $10^{12}\,\mathrm{cm}^{-3}$ permit mass separation while keeping the radial losses at acceptable levels for at least the geometric configuration considered and for ion temperatures of a few tens of eV. Since a higher ion temperature decreases the collision rate, a given ion flux distribution (light and heavy element side collection, radial losses) can theoretically be obtained at higher number density. However, the higher the ion temperature, the higher is the rotation speed required to ensure the ion confinement on the light side. A downside of operating the device at higher rotation speed is the larger associated initial kinetic energy of ions in the rotating frame, leading to larger Larmor radii, which eventually increases the radial losses. The radial losses therefore limit both the achievable number densities and ion temperature; ion temperatures of about 20 eV have been numerically shown to present a good compromise for a $8\,\mathrm{km\,s}^{-1}$ rotation speed.

For these nominal operating parameters, numerical simulations indicate that separation factors of about 2.3 can be obtained in a single pass in separating Aluminum ions from Strontium ions, while limiting the radial losses to less than 15%. These results are found for an unoptimized geometric configuration of 0.5 m in radius and 0.6 m in length. It would stand to reason that optimizing the magnetic field shape, or making the device larger in radius, would reduce the fraction of ions lost radially. This enhancement could then be used either to operate the system at larger number densities or higher separation factors for a given fraction of radial losses; or to minimize the radial losses for a given number density. Although the figure of merit for optimization would depend on the specific application considered, higher separation factors would limit the number of units to stage in order to achieve a given separation.

While the results presented in this paper clearly demonstrate the existence of a mass separation effect and give insights of the physical mechanism delimiting the operating parameter space, it certainly remains to address various practical issues before designing testing experiments. Indeed, this study highlights key questions for the design of future systems. Among these are where and how to inject particles, how to minimize radial losses while maximizing densities and how to optimize the operating conditions in response to a given plasma composition.

ACKNOWLEDGMENTS

This work was supported by US DOE Contract No. DE-AC02-09CH11466. One of us (RG) was supported by Ecole Polytechnique Graduate School and ENSTA FDO fellowships.

[1]B. Lehnert, Nucl. Fusion **11**, 485 (1971).
[2]B. Bonnevier, Ark. Fys. **33**, 255 (1966).
[3]M. Krishnan, M. Geva, and J. L. Hirshfield, Phys. Rev. Lett. **46**, 36 (1981).
[4]M. Grossman and T. Shepp, IEEE Trans. Plasma Sci. **19**, 1114 (1991).
[5]J.-M. Rax, J. Robiche, and N. J. Fisch, Phys. Plasmas **14**, 043102 (2007).
[6]T. Ohkawa and R. L. Miller, Phys. Plasmas **9**, 5116 (2002).
[7]R. Freeman, S. Agnew, F. Anderegg, B. Cluggish, J. Gilleland, R. Isler, A. Litvak, R. Miller, R. O'Neill, T. Ohkawa, S. Pronko, S. Putvinski, L. Sevier, A. Sibley, K. Umstadter, T. Wade, and D. Winslow, AIP Conf. Proc. **694**, 403 (2003).
[8]A. J. Fetterman and N. J. Fisch, Phys. Plasmas **18**, 094503 (2011).
[9]A. J. Fetterman and N. J. Fisch, Phys. Plasmas **18**, 103503 (2011).
[10]G. Abdrashitov, A. Beloborodov, V. Volosov, V. Kubarev, Y. Popov, and Y. Yudin, Nucl. Fusion **31**, 1275 (1991).
[11]A. J. Fetterman and N. J. Fisch, Phys. Rev. Lett. **101**, 205003 (2008).
[12]K. Miyamoto, *Fundamentals of Plasma Physics and Controlled Fusion* (Iwanami Book Service Center, 1997).
[13]W. M. Manheimer, M. Lampe, and G. Joyce, J. Comput. Phys. **138**, 563 (1997).
[14]C. K. Birdsall, IEEE Trans. Plasma Sci. **19**, 65 (1991).
[15]R. Phaneuf, R. Janev, and H. Hunter, Nucl. Fusion **27**, 7 (1987).
[16]J. Berland, C. Bogey, and C. Bailly, Comput. Fluids **35**, 1459 (2006).